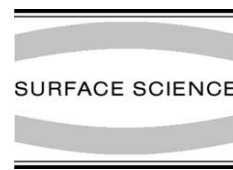




Available online at www.sciencedirect.com

SCIENCE @ DIRECT®

Surface Science 583 (2005) L135–L141



www.elsevier.com/locate/susc

Surface Science Letters

Electron-stimulated desorption from an unexpected source: Internal hot electrons for Br–Si(100)-(2 × 1)

B.R. Trenhaile, V.N. Antonov, G.J. Xu, Koji S. Nakayama, J.H. Weaver *

Department of Physics, Department of Materials Science and Engineering, and Frederick Seitz Materials Research Laboratory, University of Illinois at Urbana-Champaign, Urbana, IL 61801, United States

Received 14 February 2005; accepted for publication 6 March 2005

Available online 14 April 2005

Abstract

The desorption of Br adatoms from Br-saturated Si(100)-(2 × 1) was studied with scanning tunneling microscopy as a function of dopant type, dopant concentration, and temperature for 620–775 K. Analysis yields the activation energies and prefactors for desorption, and the former correspond to the energy separation between the Fermi level and Si–Br antibonding states. Thus, electron capture in long-lived states results in Br expulsion via a Franck–Condon transition. Analysis of the prefactors reveals that optical phonons provide the energy needed for the electronic excitation. These results show that desorption induced by an electronic transition can occur in closed system without external stimulus, and they indicate that thermally-excited charge carriers may play a general role in surface reactions.

© 2005 Elsevier B.V. All rights reserved.

Keywords: Scanning tunneling microscopy; Desorption induced by electronic transitions; Thermal desorption; Br–Si(100)-(2 × 1)

There is rich literature that describes electron- and photon-stimulated desorption from surfaces [1,2]. In general, the capture of an electron or hole in a long-lived state results in a Franck–Condon transition and the repulsive potential associated with the excited configuration leads to atom ejection. Recent investigations of clean Si(100), Si(111), and GaAs(110) demonstrated that elec-

tron and photon bombardment could cause atom ejection into the vacuum and onto the terrace [3–6]. Other studies have shown that incident electrons can cause desorption of adsorbates from semiconductor surfaces [7–9]. To our knowledge, the captured carriers have always been generated by incident electrons or photons. Indeed, there has been a clear distinction between processes that are thermally-activated and those that are electron-activated.

In this paper, we demonstrate that internal thermally-activated electrons can induce

* Corresponding author. Tel.: +1 2172443528; fax: +1 2173332736.

E-mail address: jhweaver@uiuc.edu (J.H. Weaver).

desorption of Br atoms from Br-saturated Si(100)-(2 × 1) at temperatures ranging from 620–775 K. Br–Si(100) is ideal to show a connection between phonons and electronic processes because Br is tightly bound and the known reactions that lead to desorption involve SiBr₂ and occur at much higher temperature than studied here (~950 K) [10]. The results are important because they show that an electronic transition can induce desorption in a closed system without external stimulus. Hot carriers may activate a wide range of processes which had previously gone unnoticed.

With scanning tunneling microscopy, STM, we measured the Br coverage before and after a thermal cycle and deduced the temperature-dependent desorption rate as a function of the doping concentration and type. We then determined the activation energies for desorption and found that they are in good agreement with the separation between the Si–Br antibonding, σ^* , states and the Fermi level, E_F . We conclude that desorption is caused by localization of electrons in the σ^* states. Moreover, analysis of the prefactors indicates that the optical phonons of Si are the energy source for electron excitation, and it reveals a compensation effect that arises from the entropy associated with the multiphonon excitations.

The experiments were carried out in an ultrahigh vacuum system with a base pressure of 4×10^{-11} Torr. The Si wafers were p-type (B doped, $\sim 0.010 \Omega\text{-cm}$ corresponding to $7 \times 10^{18} \text{cm}^{-3}$, denoted p-Si) and n-type (P doped, $\sim 0.5 \Omega\text{-cm}$, $9 \times 10^{15} \text{cm}^{-3}$, denoted ldn-Si for lightly-doped n-Si and $\sim 0.005 \Omega\text{-cm}$, $1 \times 10^{19} \text{cm}^{-3}$, denoted hdn-Si for heavily-doped n-Si). Clean surfaces were prepared using thermal treatments [11] and imaged to verify surface quality. They were then exposed to a flux of Br₂ to achieve surface saturation where one Br atom is bonded to each dangling bond of the (2 × 1) surface. Thereafter, they were heated to a specific temperature in the range 620–775 K for 20–90 min, cooled, and imaged at room temperature.¹ The amount of Br lost was determined from the number of bare sites per unit area [12]. The

¹ The temperature was monitored with an optical pyrometer calibrated with a W-Re thermocouple; heating rate 2K s^{-1} ; reproducibility $\pm 5 \text{K}$.

imaging conditions had no effect on the Br concentration, as concluded from repetitive same-area scanning.

Fig. 1(a) is representative of as-exposed Br–Si(100). The dimer rows are bright and they are separated by dark lines. There is one dimer vacancy, DV, and it appears as a dark feature that spans the dimer row. There are four features with one adatom missing, and these single Br vacancies, BrVs, appear dark on one side of the dimer row [13]. The Br coverage is then 0.997 ML. While BrVs can be found for samples dosed at room temperature, they convert to vacancy pairs after mild annealing, producing bare dimers, BDs.² Fig. 1(b) and (c) are representative of nearly-saturated surfaces after a 20 min anneal at 725 K. Fig. 1(b) is a filled-state image for p-Si and, again, the dimer rows are separated by dark lines. Fig. 1(c) is an empty-state image for heavily-doped n-Si where now the tunneling minimum appears in the center of the dimer rows.³ The BDs appear as symmetric features involving three dimers against a grey background—a Br-free dimer in the middle with two bright, Br-terminated dimers on either side. These triplets reflect the coupling of localized states of the BD with adjacent Si–Br levels, and their appearance varies with imaging conditions [12]. From results like those of Fig. 1, we can determine the amount of Br desorption.⁴

To describe the desorption kinetics, one must first know whether the products are atoms or molecules. The products can be deduced with STM because the vacancies produced by desorption can be frozen-in by a quench to room temperature. Images acquired after 90 min at 620–660 K always revealed both BrVs and BDs. We conclude that Br atoms are the desorption products and that subsequent vacancy diffusion produced vacancy pairs.²

² Pairing is favored by $\exp(\frac{E}{k_B T}) \sim 10^4$ at 700 K where E is the π bond energy of $\sim 0.5 \text{eV}$.

³ It is difficult to obtain filled-state images of n-Si.

⁴ For most temperature–time sequences, the final coverage was high enough that Br desorption was the only reaction that occurred. For a few sequences, the coverage decreased enough that a small amount of roughening was observed. No silicon was lost as SiBr₂ because the number of adatoms was equal to the increase in DVs.

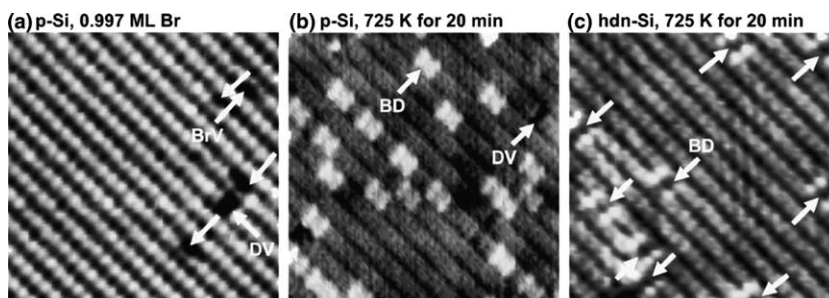


Fig. 1. (a) Filled-state image of Si(100)-(2×1) after passivation with Br at room temperature ($100 \times 100 \text{ \AA}^2$, -1.3 V). Single Br vacancies (BrVs) appear as dark spots on one side of a dimer, indicated by arrows perpendicular to the dimer row. A terrace dimer vacancy (DV) appears as a dark dimer-sized feature. (b) Filled-state image for p-Si ($100 \times 100 \text{ \AA}^2$, -0.6 V). The bright features involving three dimers are the signature of a bare dimer (BD). The initial and final coverages were 0.995 and $0.958 \pm 0.003 \text{ ML}$, giving an average desorption rate of $3.1 \times 10^{-5} \text{ ML s}^{-1}$. Desorption occurred without Si removal. (c) Empty-state image for heavily-doped n-Si ($100 \times 100 \text{ \AA}^2$, $+1.3 \text{ V}$). The tunneling minimum now appears in the center of the dimer row but BDs still appear as triplets with bright features on either side of the Br-free dimer as indicated by arrows. The initial and final coverages were 0.996 and $0.974 \pm 0.003 \text{ ML}$, giving an average desorption rate of $1.8 \times 10^{-5} \text{ ML s}^{-1}$.

Moreover, the ratio of single to paired vacancies decreased with increasing temperature, consistent with a greater diffusion length at higher temperature.

Experiments like those leading to Fig. 1 were done for each sample type at multiple temperatures following the protocol described above. From analysis of first-order Arrhenius plots, we deduced activation energies that are much lower than the Si–Br bond strength of $\sim 3.8 \text{ eV}$ [14] and prefactors much smaller than a typical attempt frequency of $\sim 10^{13} \text{ s}^{-1}$. This indicates that desorption is not thermally-activated Si–Br bond breaking. We argue below that the underlying processes are electron-activated.

Atomic desorption follows first order kinetics with the rate being

$$r = -\frac{d\theta}{dt} = k\theta \quad (1)$$

where k is the rate constant, θ is the Br concentration, and t is time. Assuming that desorption is electronically-activated and involves electron localization in the Si–Br antibonding level at energy E_{σ^*} , the rate constant is $k = IP$ where I is the electron capture rate in units of s^{-1} . Capture produces a state with one extra electron via a Franck–Condon transition, and the probability that this state will lead to Br desorption is P . From Eyring theory [15],

$$I = A \exp\left(\frac{-\Delta G}{k_B T}\right) \quad (2)$$

where A is a constant and $\Delta G = \Delta H - T\Delta S$ is the difference in free energy between the ground state and the excited state with an electron in σ^* . The change in entropy, ΔS , can be split into three parts—one associated with adding an electron to the σ^* state, ΔS_e , one associated with the phonons involved in the excitation process, ΔS_{pho} , to be discussed below, and one associated with any other changes in the molecular reaction, ΔS_{other} , presumed to be the same for each sample. ΔS_e can be related to the chemical potential, μ , through the thermodynamic relation, $\mu = -T \frac{\Delta S_e}{\Delta N}$, where $\Delta N = -1$ is the change in the number of electrons. Moreover, the enthalpy $\Delta H \approx \Delta E = E_{\sigma^*}$ where we have defined $E = 0$ for the ground state. Thus, the capture rate can be written

$$I = A \exp\left(\frac{\Delta S_{\text{pho}} + \Delta S_{\text{other}}}{k_B}\right) \exp\left(-\frac{E_{\sigma^*} - \mu}{k_B T}\right) \quad (3)$$

where $\mu = E_F$. The rate constant is then

$$k = \nu \exp\left(-\frac{\varepsilon}{k_B T}\right) \quad (4)$$

where $\nu = PA \exp\left(\frac{\Delta S_{\text{pho}} + \Delta S_{\text{other}}}{k_B}\right)$ is the prefactor and $\varepsilon = |E_{\sigma^*} - E_F| \gg k_B T$ is the activation energy. From Eq. (1),

$$\ln k = \ln \left[\frac{1}{t} \ln \left(\frac{\theta_i}{\theta_f} \right) \right] = -\frac{\varepsilon}{k_B T} + \ln v \quad (5)$$

Equation (5) is important because θ_i , θ_f , and t are known in each experiment. Fig. 2 then summarizes the rate constants, k , deduced for differently-doped Si using Eq. (5). From straight-line fits, we find that $\varepsilon_p = 1.23 \pm 0.08$ eV with $v_p = 10^{4.0 \pm 0.5} \text{ s}^{-1}$, $\varepsilon_{\text{ldn}} = 0.84 \pm 0.09$ eV with $v_{\text{ldn}} = 10^{1.0 \pm 0.5} \text{ s}^{-1}$, and $\varepsilon_{\text{hdn}} = 0.50 \pm 0.11$ eV with $v_{\text{hdn}} = 6 \times 10^{-2.0 \pm 0.9} \text{ s}^{-1}$. The desorption rates are nearly the same in the range 650–750 K, but they would be quite different at higher or lower temperature as can be deduced from Fig. 2.

If the proposed hot-electron-capture mechanism is correct, then the activation energy must track the movement of E_F . Fig. 3 shows a schematic band diagram for Br–Si(100) with the relevant energy levels at 700 K. It does not include the entropy components associated with excitation of an electron into the σ^* levels. The distribution of empty states deduced from scanning tunneling spectroscopy, STS, is shown above the conduction band minimum, CBM. The lowest feature arises from Si backbonds, and low-temperature STS on p-Si showed the σ^* levels 1.3–2.0 eV above E_F , where E_F was very close to the valence band max-

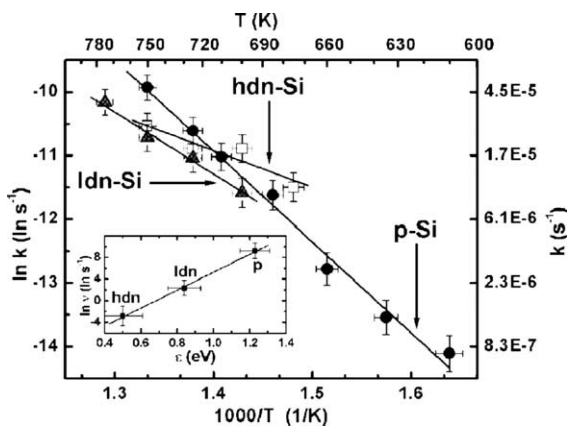


Fig. 2. Arrhenius plots for p-Si and for lightly- and heavily-doped n-Si, from which the kinetic parameters describing Br desorption were determined. The inset shows an exponential increase in v that accompanies an increase in ε . The inverse of the slope, Δ_0 , is 60 ± 5 meV and this characteristic energy indicates that the optical phonons of Si are the energy pool needed for electron excitation.

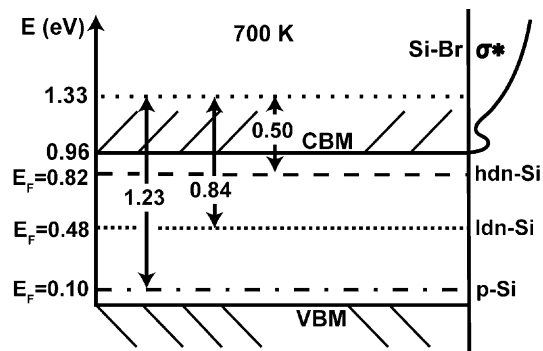


Fig. 3. Energy level picture for Si at 700 K. The Fermi levels are indicated by the dashed lines, and the energy scale is shown on the left, with the VBM taken to be $E = 0$. Also depicted are Si states near the CBM and Si–Br σ^* -derived states that start ~ 1.1 eV above the VBM. The double-headed arrows depict the activation energies deduced from Fig. 2. Electron capture in the σ^* states occurs for all samples, but a shift in the Fermi level changes the internal energy of the reaction.

imum, VBM. To locate them at 700 K, we assumed that the $\sigma - \sigma^*$ separation had the same temperature dependence as the band edges so that σ^* moved with the CBM [16].⁵ As shown, E_F is about 0.10 eV above the VBM for p-Si at 700 K, assuming non-degenerate doping. It is 0.48 and 0.82 eV above the VBM for lightly- and heavily-doped n-Si. The bands are drawn flat since Br adsorption eliminates the surface states in the gap [17–19]. This has been confirmed through low-temperature STS where E_F shifted toward the CBM from p- to n-Si.

Fig. 2 showed that the excitation energies needed to desorb Br from p-Si, ldn-Si, and hdn-Si were $\varepsilon_p = 1.23 \pm 0.08$ eV, $\varepsilon_{\text{ldn}} = 0.84 \pm 0.09$ eV, and $\varepsilon_{\text{hdn}} = 0.50 \pm 0.11$ eV, respectively. The double-headed arrows in Fig. 3 show that excitations with these energies could result in electron capture in Si–Br σ^* states. Significantly, the changes in these values are in excellent agreement with the Fermi level shift associated with doping, again implicating the σ^* states.

After electron capture, Br desorption proceeds through the mechanisms described by conven-

⁵ Pankove [16] discussed the temperature dependence of semiconductor band gaps. For silicon, the bulk band gap decreases from 1.00 eV at 620 K to 0.93 eV at 775 K.

tional electron-stimulated desorption [1]. Determination of excited state lifetimes and the detailed ejection pathway would require extensive theoretical analysis that is beyond the scope of this study. Although, to our knowledge, no calculation of lifetimes for excited states of Br–S(100) have been undertaken, a previous study showed that capture of an electron in the σ^* states induced Br hopping at room temperature [13]. If the state is sufficiently long-lived to cause hopping, it should also be sufficient to induce atom ejection at higher temperature.

Insight into the underlying thermodynamics of desorption can be gained by analysis of the prefactors. From experiment, ν spans almost six orders of magnitude which, at first glance, seems difficult to rationalize since the samples are the same except for their doping. The variation in the prefactors follows naturally, however, if we return to Eq. (3) and recognize the significance of the entropy term, $\exp(\frac{\Delta S_{\text{pho}}}{k_B})$, included in the prefactor. The Eyring model describes activation as a change in Gibbs free energy, not simply the change in enthalpy or internal energy. The observation that an increase in ϵ is compensated by an exponential increase in ν is well known from the literature of biological, chemical, and physical processes as the Meyer–Neldel rule [20,21].

The Meyer–Neldel rule states that for groups of related processes whose rate constants are given by Eq. (4), the prefactor and activation energy are related by

$$\ln \nu = a + b\epsilon \quad (6)$$

where a and b are positive constants. Peacock-Lopez and Suhl [22], and later Yelon and Movaghar (YM) showed that the compensation effect can be obtained by counting the number of ways in which the heat bath can supply the elementary excitations (phonons) necessary to overcome the activation energy. It was shown that compensation is expected when the activation energy for a reaction is large compared to $k_B T$ and to the elementary excitations of the system [21,23]. From the YM model, $\Delta_0 = \frac{1}{b}$ gives an order of magnitude estimate of the energy that is characteristic of the relevant elementary excitations [24]. From the Meyer–Neldel rule, one can expect a cross-over

in the rates at some isokinetic temperature, T_{iso} , that is given by $\frac{\Delta_0}{k_B}$. From Fig. 2, we see rate crossings at ~ 700 K and a common point is within experimental uncertainty.

The inset of Fig. 2 shows $\ln \nu$ vs. ϵ for hot-electron induced desorption from Br–Si(100). From the best fit, $\Delta_0 = 60 \pm 5$ meV. From the YM model, Δ_0 depends on both the phonon frequency and the electron–phonon coupling constant. While an exact prediction of the energy would require the coupling constant for multiphonon processes in silicon, our value is consistent with what has been observed for processes attributed to coupling with the optical phonon bath. In particular, Yelon et al. fitted the data for experiments on deep trapping in crystalline silicon and found a Δ_0 value of 50 ± 25 meV [21]. They also showed that values of Δ_0 in the range of 35–70 meV are plausible for coupling to optical phonons for semiconductors with bandgaps of 1–2 eV [20,21]. Thus, we conclude that the optical-phonon bath provides the energy for the electronic excitation.

We emphasize that the cross-over point is usually inferred from extrapolation of Arrhenius plots, and the actual observation of the cross-over provides strong evidence that the compensation effect did not arise from errors in data collecting. Cross-over is only possible if the localized σ^* states are thermodynamically inseparable from the phonons due to their strong coupling to the lattice. This implies a transition to a thermodynamic state defined by the excited Si–Br bond and the phonon population in a certain interaction volume, rather than a simple electronic transition over a barrier ϵ . While we cannot further specify the details of the mechanism for the multiphonon excitation process, we speculate that the process is similar to the models proposed for multiphonon carrier transitions in semiconductors. These models involve the capture of excited carriers by defect states that are strongly coupled to the lattice [25,26].

Fig. 4 is a schematic of hot-electron capture. The wavy lines represent phonons combining to give the electron the energy needed to reach the σ^* state. Excitation occurs in some interaction volume around the Si–Br bond and can, in principle, come from any occupied level. The number of

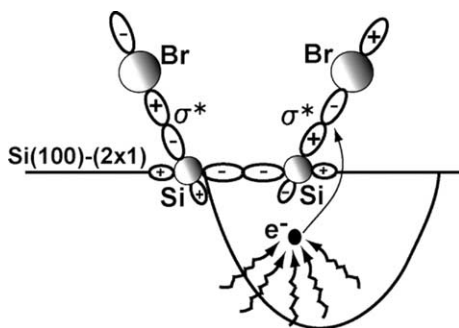


Fig. 4. A schematic of multiphonon excitation of an electron into a σ^* state from within an interaction volume around the Si–Br bond. The excitation rate includes an entropy term that describes the way that phonons can assemble to provide the needed energy. The entropy compensates the change in $(E_{\sigma^*} - E_F)$ caused by doping. Capture can result in Br desorption via a Franck–Condon transition.

phonons required depends on the internal energy of the electron relative to σ^* . The electronic transitions are not the same for p- and n-Si because doping shifts the chemical potential. This shift is compensated by a corresponding change in entropy, ΔS_{pho} , associated with the number of ways the phonons can assemble to provide the needed energy. The electron transition rate is determined by competition between entropy and the chemical potential, and, for $T > T_{\text{iso}}$, this rate becomes greater for p-Si, leading to a higher Br desorption rate.⁶

Hot-electron stimulated desorption also provides an answer to an important question related to roughening/etching of Si(100). The reaction sequence in both cases calls for the transfer of a halogen atom from one Si atom of a surface dimer to the other, followed by the transfer of the first Si atom onto the terrace and then the desorption of the SiBr_2 species (etching) or the transfer of the halogen atoms and the remaining Si atom to the terrace (roughening) [27,28]. Roughening/etching requires bare dimers, and saturated surfaces have none. Nonetheless, a saturated surface does roughen, albeit slowly, at elevated temperature [12,29]. From the above discussion, ESD provides the needed

⁶ Detailed balance does not apply because electron excitation and capture are irreversible.

mechanism for creation of bare dimers—and allows the surface to undergo other reactions.

We have shown that desorption can be induced by thermally-activated internal electrons. The broader implication is that one should expect thermally-excited carriers to activate a wide variety of reactions. For complex reaction sequences, as in catalysis, it is likely that they contribute at several stages to processes that have been attributed to thermal bond modification. From this perspective, electronic and thermal processes are inseparable. In desorption, for example, the phonons play a dual role by weakening the adatom-surface bond through vibrations and by providing the free energy needed for electron excitation.

Acknowledgements

We thank A. Yelon, R.S. Crandall, C.M. Aldao, Abhishek Agrawal, and A.W. Signor for stimulating discussions. This work was supported by the National Science Foundation. V.N. Antonov was supported by the Department of Energy under Award No. DEFG02-91-ER45439 through the Frederick Seitz Materials Research Laboratory at the University of Illinois.

References

- [1] R.D. Ramsier, J.T. Yates Jr., Surf. Sci. Rep. 12 (1991) 243, and references therein.
- [2] T.E. Madey, Surf. Sci. 299/300 (1994) 824, and references therein.
- [3] J. Kanasaki, T. Ishida, K. Ishikawa, K. Tanimura, Phys. Rev. Lett. 80 (1998) 4080.
- [4] K. Nakayama, J.H. Weaver, Phys. Rev. Lett. 82 (1999) 980.
- [5] B.Y. Han, K. Nakayama, J.H. Weaver, Phys. Rev. B 60 (1999) 13846.
- [6] J. Kanasaki, M. Nakamura, K. Ishikawa, K. Tanimura, Phys. Rev. Lett. 89 (2002) 257601.
- [7] T.-C. Shen, C. Wang, G.C. Abeln, J.R. Tucker, J.W. Lyding, Ph. Avouris, R.E. Walkup, Science 268 (1995) 1590.
- [8] E.T. Foley, A.F. Kam, J.W. Lyding, Ph. Avouris, Phys. Rev. Lett. 80 (1998) 1336.
- [9] K. Mochiji, M. Ichikawa, Phys. Rev. B 63 (2001) 115407.
- [10] M.C. Flowers, N.B.H. Jonathan, Y. Liu, A. Morris, Surf. Sci. 343 (1995) 133.

- [11] K. Hata, T. Kimura, S. Ozawa, H. Shigekawa, *J. Vac. Sci. Technol. A* 18 (2000) 1933.
- [12] G.J. Xu, E. Graugnard, B.R. Trenhaile, K.S. Nakayama, J.H. Weaver, *Phys. Rev. B* 68 (2003) 075301.
- [13] K.S. Nakayama, E. Graugnard, J.H. Weaver, *Phys. Rev. Lett.* 89 (2002) 266106.
- [14] D.R. Lide (Ed.), *CRC Handbook of Chemistry and Physics*, 75th ed., CRC Press, 1995.
- [15] S. Glasstone, K.J. Laidler, H. Eyring, *The Theory of Rate Processes*, McGraw-Hill, New York, 1941.
- [16] J.I. Pankove, *Optical Processes in Semiconductors* Dover, New York, 1971.
- [17] R.J. Hamers, P. Avouris, F. Bozso, *Phys. Rev. Lett.* 59 (1987) 2071.
- [18] L. Liu, J. Yu, J.W. Lyding, *Appl. Phys. Lett.* 78 (2001) 386.
- [19] L. Liu, J. Yu, J.W. Lyding, *IEEE Trans. Nanotechnol.* 1 (2002) 176.
- [20] R.S. Crandall, *Phys. Rev. B* 66 (2002) 195210, and references therein.
- [21] A. Yelon, B. Movaghar, H.M. Branz, *Phys. Rev. B* 46 (1992) 12244, and references therein.
- [22] E. Peacock-Lopez, H. Suhl, *Phys. Rev. B* 26 (1982) 3774.
- [23] A. Yelon, B. Movaghar, *Phys. Rev. Lett.* 65 (1990) 618.
- [24] G. Boisvert, L.J. Lewis, A. Yelon, *Phys. Rev. Lett.* 75 (1995) 469.
- [25] J.S. Blakemore, *Semiconductor Statistics*, Pergamon Press, New York, 1962, and references therein.
- [26] C.H. Henry, D.V. Lang, *Phys. Rev. B* 15 (1977) 989, and references therein.
- [27] Koji Nakayama, C.M. Aldao, J.H. Weaver, *Phys. Rev. Lett.* 82 (1999) 568.
- [28] Koji Nakayama, C.M. Aldao, J.H. Weaver, *Phys. Rev. B* 59 (1999) 15893.
- [29] Dongxue Chen, John J. Boland, *Phys. Rev. B* 67 (2003) 195328.